Neurobiology of Aging 65 (2018) 41–50

Contents lists available at ScienceDirect

Neurobiology of Aging

journal homepage: www.elsevier.com/locate/neuaging

Hypermetabolism in the hippocampal formation of cognitively impaired patients indicates detrimental maladaptation

Ivayla Apostolova [a,b,2], Catharina Lange [c,2], Anja Mäurer [d], Per Suppa [e], Lothar Spies [e], Michel J. Grothe [f], Till Nierhaus [g,h], Jochen B. Fiebach [i], Elisabeth Steinhagen-Thiessen [j], R. Buchert [b,c,*], for the Alzheimer's Disease Neuroimaging Initiative [1]

[a] Department of Radiology and Nuclear Medicine, University Hospital Magdeburg, Magdeburg, Germany
[b] Department of Nuclear Medicine, University Hospital Hamburg-Eppendorf, Hamburg, Germany
[c] Department of Nuclear Medicine, Charité - Universitätsmedizin Berlin, Berlin, Germany
[d] Evangelisches Geriatriezentrum Berlin, Berlin, Germany
[e] jung diagnostics GmbH, Hamburg, Germany
[f] German Center for Neurodegenerative Diseases (DZNE), Rostock, Germany
[g] Department of Neurology, Max Planck Institute for Human Cognitive and Brain Sciences, Leipzig, Germany
[h] Center for Cognitive Neuroscience Berlin (CCNB), Department of Education and Psychology, Freie Universität Berlin, Germany
[i] Center for Stroke Research Berlin, Charité–Universitätsmedizin, Berlin, Germany
[j] Lipid Clinic at the Interdisciplinary Metabolism Center, Charité - Universitätsmedizin, Berlin, Germany

ARTICLE INFO

Article history:
Received 26 July 2017
Received in revised form 27 December 2017
Accepted 7 January 2018
Available online 31 January 2018

Keywords:
Hippocampal formation
Hypermetabolism
Cognitive impairment
Dementia
Geriatric inpatients
Positron emission tomography

ABSTRACT

Structural deterioration and volume loss of the hippocampal formation is observed in many diseases associated with memory decline. Paradoxically, glucose metabolism of the hippocampal formation can be increased at the same time. This might be a consequence of compensatory (beneficial) or maladaptive (detrimental) mechanisms. Aim of this study was to differentiate between compensation and maladaptation by analyzing the association between glucose metabolism in the hippocampal formation measured by positron emission tomography with the glucose analogue 18F-fluorodeoxyglucose and cognitive performance as characterized by the extended Consortium to Establish a Registry for Alzheimer's Disease test battery in a sample of 87 patients (81.8 ± 5.4 years) with mild cognitive impairment or mild dementia and varying etiological diagnoses. Glucose metabolism in the hippocampal formation was negatively correlated with the performance in several cognitive subdomains, most pronounced for verbal semantic fluency, independent of overall neuronal dysfunction, presence of clinical Alzheimer's disease, and overall cognitive performance. This finding provides evidence that increased glucose metabolism in the hippocampal formation of cognitively impaired patients indicates detrimental maladaptation rather than a beneficial compensatory reaction. Excess glucose metabolism in the hippocampal formation might be a useful therapeutic target in these patients.

© 2018 Elsevier Inc. All rights reserved.

1. Introduction

The hippocampus is a key brain region in the pathogenesis of memory dysfunction in many diseases including Alzheimer's disease (AD) (Schroder and Pantel, 2016), frontotemporal lobar degeneration (Dermody et al., 2016), Parkinson's disease (Gee et al., 2017), and also non-neurodegenerative diseases such as depression (den Heijer et al., 2011). Hippocampal atrophy is also observed in cerebrovascular disease (CVD), in line with selective vulnerability of the hippocampus in brain ischemia-hypoxia (Schmidt-Kastner and Freund, 1991). In AD, the hippocampus is among the first targets for tau tangle aggregates (after the transentorhinal cortex) (Braak and Braak, 1991) and shows impaired functional connectivity (Brier et al., 2012; Petrella et al., 2011; Zhang et al., 2010) and atrophy (Jack et al., 1999). Atrophy of the hippocampus and other mesiotemporal structures is a very consistent finding in AD and its prodromal stages (Chapleau et al., 2016), and therefore, it is considered a very promising biomarker to support the etiological diagnosis of AD in subjects with mild cognitive impairment (MCI; Ten Kate et al., 2017). Mental and physical training can stimulate neurogenesis in

* Corresponding author at: Martinistr. 52, 20246 Hamburg, Germany. Tel.: +49 40 7410 54347; fax: +49 40 7410 40265.
E-mail address: r.buchert@uke.de (R. Buchert).

[1] Some of the data used in preparation of this article were obtained from the Alzheimer's Disease Neuroimaging Initiative (ADNI) database (adni.loni.usc.edu). As such, the investigators within the ADNI contributed to the design and implementation of ADNI and/or provided data but did not participate in analysis or writing of this article. A complete listing of ADNI investigators can be found at http://adni.loni.usc.edu/wp-content/uploads/how_to_apply/ADNI_Acknowledgement_List.pdf.

[2] These authors contributed equally.

0197-4580/$ – see front matter © 2018 Elsevier Inc. All rights reserved.
https://doi.org/10.1016/j.neurobiolaging.2018.01.002

the hippocampus resulting in gain of hippocampal gray matter (GM) volume, detectable by magnetic resonance imaging (MRI), and improvement of memory function (DiFeo and Shors, 2017; Duzel et al., 2016).

Positron emission tomography (PET) of the brain with the glucose analogue 18F-fluorodeoxyglucose (FDG) is a well-established functional imaging modality for noninvasive in vivo assessment of brain glucose metabolism as surrogate marker of signaling-related synaptic activity (Sokoloff, 1999). Dysfunction and loss of synapses in AD results in a characteristic spatial pattern of reduced FDG uptake in the brain comprising the posterior cingulate cortex/precuneus area and parietotemporal association cortices (Minoshima et al., 1997). Other diseases present with different reduction patterns in FDG PET, which is the rationale for the use of FDG PET in the differential diagnosis of dementing diseases. FDG PET can detect the disease characteristic alterations of brain activity before cognitive decline is recognized (Terry et al., 1991).

In striking contrast to the very consistent association between mesiotemporal atrophy and memory decline, mesiotemporal FDG PET findings in patient populations with memory decline are far from being consistent. Some groups reported reduced hippocampal FDG uptake in AD (De Santi et al., 2001; Ishii et al., 1996; Mosconi et al., 2005, 2006; Nestor et al., 2003). Other authors reported rather preserved or even increased hippocampal glucose metabolism despite hippocampal atrophy and suggested compensation mechanisms to maintain function by recruiting additional neuronal resources as possible explanation (Chetelat et al., 2008; Desgranges et al., 1998; Herholz et al., 2002; Ibanez et al., 1998; Ishii et al., 1998; Minoshima et al., 1997). A functional resting-state MRI (rs-fMRI) study by Tahmasian et al. (Tahmasian et al., 2015) using seed-based functional connectivity analysis recently revealed hippocampal glucose metabolism to be inversely correlated with the connectivity of hippocampus and precuneus. This finding supports the hippocampus disconnection hypothesis according to which uncoupling from cortical inputs might cause increased hippocampal activity (Das et al., 2013; Pasquini et al., 2015; Tahmasian et al., 2015).

There is not only ongoing discussion of quite different mechanisms that might contribute to hippocampal hyperactivity in cognitive decline but also it is even not clear whether hippocampal hyperactivity results from compensatory or maladaptive alterations (Pievani et al., 2014). Yet, compensatory mechanisms, for example, recruitment of additional neuronal resources, are expected to improve cognition, whereas maladaptation should result in further deterioration of cognitive performance compared to patients with the same level of neuropathology but hippocampal glucose metabolism decreasing in parallel with hippocampus volume. To test whether relative increase of hippocampal glucose metabolism is due to compensatory (beneficial) or maladaptive (detrimental) mechanisms, this study evaluated the association between glucose metabolism in the hippocampal formation and cognitive performance in a sample of 87 patients with MCI or mild dementia of diverse etiology hospitalized in a geriatrics unit for an acute or subacute indication (the hippocampal formation was used rather than the hippocampus because this larger region of interest better matches the spatial resolution of PET). In addition, the study assessed the relationship between glucose metabolism in the hippocampal formation and corticohippocampal connectivity as assessed by rs-fMRI using very similar analysis methods as the study by Tahmasian et al. (2015), to simplify comparison of the results. Brain FDG PET, rs-fMRI, and detailed neuropsychological testing had been performed as part of a prospective study (WHO Trials Registry DRKS00005041) (Apostolova et al., 2017; Ritter et al., 2016). This clinical patient sample was expected to cover a large range of FDG uptake in the hippocampal formation (HippForm-FDG) and, therefore, to provide adequate power to detect possible associations between glucose metabolism and cognitive performance.

2. Material and methods

2.1. Cognitively impaired patients

The sample of cognitively impaired patients was derived from the prospective clinical study "Comparison and integration of modalities in the early and differential diagnosis of dementing disorders in hospitalized geriatric patients: a prediction study" (WHO Trials Registry DRKS00005041). This investigator-initiated study has been approved by the German Federal Institute for Drugs and Medical Devices as phase III trial of FDG PET for the diagnosis of cognitive impairment (reference 61-3910-4039304; EudraCT 2013-000140-2). Ethics approval has been obtained from the ethics committee of the state of Berlin (13/0234-EK12). Monitoring was conducted both internally (by the Charité research group geriatrics) and externally (by syneed medidata GmbH, Konstanz, Germany). The main inclusion criterion of this study was clinically uncertain suspicion of AD, CVD, or mixed disease (MD, AD + CVD) as the cause of cognitive impairment (Apostolova et al., 2017; Ritter et al., 2016).

The analyses presented here included all patients who successfully completed FDG PET and structural MRI (i.e., T1-weighted magnetization prepared rapid acquisition gradient echo [MPRAGE]) and for whom an etiological diagnosis of their cognitive impairment by an interdisciplinary team of academic experts was available (n = 87, age = 81.8 ± 5.4 years, 57 females). The etiological diagnoses included non-neurodegenerative etiology (n = 15), AD (n = 17), CVD (n = 23), MD (n = 25), and neurodegenerative etiology other than AD (n = 7). The etiological diagnosis was based on patient history, physical/neurological examination, standard blood/urine laboratory tests, detailed neuropsychological testing, structural MRI, and FDG PET. The etiological subgroups did not differ with respect to education (duration in years, analysis of variance $p = 0.714$). The clinical dementia rating score was 0 in 2.3% of the patients, 0.5 in 63.2%, and >0.5 in 34.5% of the included patients. Patient characteristics are summarized in Table 1. The patient sample reflects the wide spectrum of diseases associated with hippocampal alterations and cognitive impairment.

Neuropsychological testing included the German version of the test battery of the Consortium to Establish a Registry for Alzheimer's Disease (CERAD; Morris et al., 1988). The CERAD test battery comprised tests of verbal fluency (by naming animals), an abbreviated version of the Boston Naming Test (15 items), Mini–Mental State Examination (MMSE), word list learning/recall/recognition, constructional praxis and recall of constructional praxis, Trail Making Test A (TMT-A), Trail Making Test B (TMT-B), and a phonemic fluency test ("S-words") (Monsch and Kressig, 2010). All subscores were transformed to z-scores corrected for age, sex, and education based on normative samples for the German CERAD version (Ehrensperger et al., 2010).

MRI of the brain was performed with a 3T MR scanner (Siemens Trio Tim) for all patients. The structural sequences included 3-dimensional T1-weighted MPRAGE ($1 \times 1 \times 1$ mm^3) and T2-weighted fluid attenuation inversion recovery (in-plane 1.2 mm, slice thickness 2.5 mm). The functional sequences included rs-fMRI based on a 2-dimensional single-shot echo-planar imaging sequence (repetition time = 2300 ms, echo time = 30 ms, $\alpha = 90°$, 64×64 matrix, 34 slices, voxel size = 3.0×3.0×4.0 mm^3, bandwidth = 2232 Hz/pixel, 1 average, segmented k-space) with 150 time points and a time resolution of 2300 ms.

Brain FDG PET was acquired with a time-of-flight PET/CT system Philips GEMINI TF 16 according to common guidelines (Varrone et al., 2009).

Table 1
Patient characteristics

Variable	All (n = 87)	AD (n = 17)	CVD (n = 23)	MD (n = 25)	Non-neurodegenerative (n = 15)	Other neurodegenerative (n = 7)
Age (years)	81.8 ± 5.4	79.6 ± 3.9	81.0 ± 6.2	84.1 ± 4.9	82.7 ± 5.4	79.1 ± 4.1
Females (n/%)	57/65.5	13/76.5	13/56.5	17/68.0	11/73.3	3/42.9
Education (years)	12.1 ± 3.5	12.4 ± 3.5	12.6 ± 3.7	12.2 ± 3.3	11.0 ± 2.7	12.2 ± 5.4
ApoE4 (one E4 allele/two E4 alleles)	25.9%/3.5% (n = 85)	38%/6%	13%/0	33%/4%	20%/7%	29%/0
HippForm-FDG	1.17 ± 0.15	1.13 ± 0.20	1.20 ± 0.12	1.17 ± 0.16	1.15 ± 0.13	1.26 ± 0.08
AD-FDG	1.95 ± 0.31	1.77 ± 0.20	2.10 ± 0.28	1.77 ± 0.21	2.19 ± 0.27	1.97 ± 0.42
HippForm-GM (mL)	5.38 ± 1.02	4.93 ± 0.94	5.60 ± 0.92	5.05 ± 0.93	5.88 ± 0.91	5.81 ± 1.38
CERAD-Plus (z-scores)						
Animals	−1.44 ± 1.10 (n = 86)	−1.79 ± 1.14	−1.50 ± 0.86	−1.70 ± 0.95	−0.31 ± 0.97	−1.94 ± 1.16
Boston Naming Test	−0.40 ± 1.33 (n = 84)	−0.74 ± 1.72	−0.51 ± 1.14	−0.31 ± 1.28	0.19 ± 1.14	−0.80 ± 1.22
MMSE	−3.53 ± 1.58 (n = 87)	−3.99 ± 1.37	−3.18 ± 1.70	−3.99 ± 1.38	−2.73 ± 1.74	−3.60 ± 1.35
Learning word list	−2.32 ± 1.48 (n = 86)	−3.15 ± 1.71	−2.22 ± 0.98	−2.44 ± 1.56	−1.61 ± 1.40	−1.79 ± 1.46
Word list intrusions	−0.94 ± 1.35 (n = 86)	−0.99 ± 1.63	−0.91 ± 1.41	−1.17 ± 1.23	−0.81 ± 1.08	−0.39 ± 1.50
Recall word list	−1.98 ± 1.17 (n=86)	−2.87 ± 0.93	−1.65 ± 0.96	−2.26 ± 1.19	−1.46 ± 1.20	−1.13 ± 0.69
Word list recognition	−1.03 ± 1.61 (n = 85)	−1.98 ± 1.73	−0.47 ± 1.60	−0.90 ± 1.52	−0.87 ± 1.35	−1.39 ± 1.50
Copy figures	−1.39 ± 1.40 (n=84)	−1.42 ± 1.04	−1.10 ± 1.36	−1.57 ± 1.21	−0.97 ± 1.06	−2.57 ± 2.67
Recall figures	−1.79 ± 1.13 (n = 84)	−2.14 ± 1.13	−1.70 ± 1.11	−2.00 ± 0.92	−1.01 ± 1.25	−2.22 ± 0.87
TMT-A	−1.28 ± 1.08 (n = 69)	−1.33 ± 1.33	−1.41 ± 0.95	−1.69 ± 0.80	−0.58 ± 1.17	−1.25 ± 0.83
TMT-B	−1.16 ± 0.88 (n = 27)	−1.27 ± 0.86	−1.23 ± 1.15	−1.65 ± 0.79	−0.65 ± 0.73	−1.55 ± 0.35
S-words	−1.08 ± 1.17 (n = 78)	−1.05 ± 1.11	−1.32 ± 1.03	−1.41 ± 0.99	−0.03 ± 1.33	−1.53 ± 0.72

Numbers are given as mean ± standard deviation of the sample.
Key: AD, Alzheimer's disease; AD-FDG, FDG uptake in the AD meta-ROI; CVD, cerebrovascular disease; FDG, 18F-fluorodeoxyglucose; HippForm-FDG, FDG uptake in the hippocampal formation; HippForm-GM, gray matter volume of the hippocampal formation; MD, mixed disease; MMSE, Mini–Mental State Examination; ROI, region of interest; TMT, Trail Making Test.

2.2. Cognitively normal control subjects

A sample of cognitively normal control (NC) subjects was obtained from the Alzheimer's Disease Neuroimaging Initiative (ADNI). For each of the 87 cognitively impaired patients, the ADNI NC subject with closest age at the time of baseline FDG PET was selected among all ADNI NC subjects with brain MRI and FDG PET at baseline. This resulted in an age-matched sample of 87 ADNI NC subjects (80.8 ± 3.2 years, t test $p = 0.160$) that was used for defining normative data for hippocampal formation FDG PET signal.

Image data itself may systematically differ between the ADNI and the group of cognitively impaired patients of the present study because of scanner-specific differences in image characteristics. However, spatial resolution in the reconstructed PET images, the most important cause of interscanner differences of (attenuation- and scatter-corrected) PET images (Joshi et al., 2009), was very similar in both samples: 8-mm full-width-at-half-maximum (FWHM) in the ADNI sample (Jagust et al., 2010) and 7-mm FWHM in the sample of cognitively impaired patients (Ritter et al., 2016). In addition, this small difference was taken into account by partial volume effect (PVE) correction (subsection "PET image analysis").

Data of the NC subjects were obtained from the ADNI database (adni.loni.usc.edu). The ADNI was launched in 2003 as a public-private partnership, led by Principal Investigator Michael W. Weiner, MD. The primary goal of ADNI has been to test whether serial MRI, PET, other biological markers, and clinical and neuropsychological assessment can be combined to measure the progression of MCI and early AD.

2.3. PET image analysis

PET images were acquired, reconstructed, and corrected for head motion as described previously (Lange et al., 2016). Correction of PVEs was performed using the Müller-Gärtner method (Muller-Gartner et al., 1992) as implemented in the PETPVE12 toolbox developed and validated by Gonzalez-Escamilla et al. (2017). The individual tissue probability maps for partial volume correction were obtained by applying the unified segmentation algorithm of the statistical parametric mapping software package (version SPM12, default parameter settings) to the individual MPRAGE MRI. PVE correction assumed spatial resolution of 8-mm and 7-mm FWHM in the ADNI sample and in the sample of cognitively impaired patients, respectively.

PVE-corrected HippForm-FDG was computed separately for the left and right hemisphere using the union of the unilateral hippocampus region of interest (ROI) and the ipsilateral parahippocampus ROI in the anatomical space of the Montreal Neurological Institute (MNI) as defined by the Automated Anatomic Labeling (AAL) atlas (Tzourio-Mazoyer et al., 2002) implemented in the WFU PickAtlas (Maldjian et al., 2003). The inverse of the elastic transformation from patient space to MNI space generated by unified segmentation was used to transform the ROIs from MNI space to patient space for ROI analysis.

PVE-corrected HippForm-FDG was scaled to mean FDG uptake in the pons. The pons ROI of the "TD Lobes" atlas in the WFU PickAtlas was used for this purpose (after transformation to patient space; Minoshima et al., 1995). FDG uptake in the pons was not corrected for PVE because the pons mainly consists of white matter (WM) tracts and the used Müller-Gärtner PVE correction algorithm is only defined for the GM of the brain (MPRAGE MRI does not allow reliable segmentation of the small GM nuclei in the pons).

The maximum over left and right hemispheres of the pons-scaled, PVE-corrected HippForm-FDG was used in the analyses presented here. The rationale for using the maximum over the left and right hippocampus (rather than the mean) was that averaging over both hemispheres dilutes the effect of hypermetabolism that is more pronounced in 1 hemisphere.

The union of the bilateral AAL-ROIs of posterior cingulate, precuneus, and inferior and superior parietal cortices was used as AD signature meta-ROI to assess pons-scaled, PVE-corrected FDG uptake in brain regions typically most affected by AD (AD-FDG).

2.4. GM volume of the hippocampal formation

GM volume of the hippocampal formation (HippForm-GM) was obtained by applying the same AAL-ROIs for the left and right

hippocampal formation used to assess FDG uptake to the patient's GM probability map from unified segmentation (in patient space). HippForm-GM was obtained by summing the voxel intensities over all voxels of the GM tissue probability map within the ROI, as described previously (Suppa et al., 2015a,b; Wolf et al., 2017). The minimum of GM volume in the left and right hippocampal formation (HippForm-GM) was used in the analyses.

2.5. Resting-state fMRI connectivity analysis

The first 5 volumes of each rs-fMRI scan were removed to account for adaptation of the patient to scanner noise and environment. FMRIB Software Library (FSL) (http://www.fmrib.ox.ac.uk/fsl) and Analysis of Functional NeuroImages (AFNI) (http://afni.nimh.nih.gov/afni) were used for slice time correction, spike removal, head motion correction, removal of the skull, and detrending. Further analysis was performed using SPM8 (www.fil.ion.ucl.ac.uk/spm/) running under MATLAB 8.2 (The MathWorks, Inc, Natick, MA). Anatomical (T1) images were coregistered to the rs-fMRI images and segmented into GM, WM, and cerebrospinal fluid (CSF). All images (GM, WM, CSF, and rs-fMRI) were spatially normalized to the MNI152 space with the voxel size $3 \times 3 \times 3$ mm^3. An average of GM, WM, and CSF mask was derived from the individual segmented GM, WM, and CSF images, respectively. Smoothing with a 6-mm Gaussian kernel (FWHM) and temporal band-pass filtering (0.01–0.1 Hz) was applied to the rs-fMRI data. CompCor analysis (DPABI—toolbox for Data Processing and Analysis of Brain Imaging, http://rfmri.org/dpabi) was performed within the CSF/WM mask on the rs-fMRI data (Behzadi et al., 2007). The resulting first 5 principal components, together with 6 head motion parameters and the global mean signal (calculated within the GM mask), were used as nuisance signals to regress out associated variance.

Eigenvector centrality maps were generated within the GM mask using fast eigenvector centrality mapping (ECM) (Lohmann et al., 2010; Wink et al., 2012). ECM is a data-driven method to characterize the connectivity of a voxel within the whole brain without any prior assumption. ECM attributes a value to each voxel in the brain that is large if the voxel is strongly correlated with many other nodes that are themselves central within the network (Lohmann et al., 2010). Eigenvector centrality of an ROI such as the hippocampal formation was obtained by averaging eigenvector centrality over all voxels in the ROI.

To further analyze whole-brain functional connectivity, rs-fMRI data were parcellated into 116 ROIs according to the AAL atlas by averaging the blood oxygenation level dependent time courses of all voxels within 1 ROI. Then Pearson's correlation coefficient between any 2 ROIs was calculated.

2.6. Statistical analyses

First, HippForm-FDG, FDG uptake in the AD meta-ROI (AD-FDG), and HippForm-GM were tested for association with each of the CERAD-Plus subscores using Pearson's correlation test.

In the second step, statistically significant correlations from the first step were corrected for overall cognitive performance (MMSE z-score), AD-FDG, or clinical diagnosis of probable AD (binary score with value 1 in case of AD or MD, value 0 in case of non-neurodegenerative etiology or neurodegenerative etiology other than AD).

Third, multivariable linear regression analysis of CERAD-Plus subscores was performed with HippForm-FDG, AD-FDG, HippForm-GM, and MMSE z-score as explanatory variables (backwards, probability-of-F-to-enter ≤ 0.05, probability-of-F-to-remove ≥ 0.10).

Finally, HippForm-FDG was tested for correlation with the eigenvector centrality of the hippocampal formation and with the connectivity of the hippocampal formation with each AAL-ROI. Eigenvector centrality and connectivity of the hippocampal formation in the same hemisphere from which HippForm-FDG was derived was used in these analyses.

3. Results

3.1. Imaging-based markers in cognitively impaired patients

HippForm-FDG ranged between 0.71 and 1.60 (mean 1.17 ± 0.15, median 1.15), AD-FDG ranged between 1.35 and 2.83 (mean 1.95 ± 0.31, median 1.89), and HippForm-GM ranged between 2.77 and 8.12 mL (mean 5.38 ± 1.02 mL, median 5.50 mL). The differences of HippForm-FDG between etiological subgroups did not reach the level of statistical significance, neither the difference between the 5 etiological subgroups according to Table 1 (Kruskal-Wallis $p = 0.139$) nor the difference between patients with AD (either alone or with concomitant CVD) and the remaining patients (1.15 ± 0.18 vs. 1.19 ± 0.12, t-test $p = 0.202$). In contrast, AD-FDG differed between etiological groups (Kruskal-Wallis $p < 0.0005$): in AD patients and in MD patients, it was lower compared to "non-neurodegenerative" patients and compared to CVD patients (all Mann-Whitney $p < 0.0005$). HippForm-GM also differed between etiological groups (Kruskal-Wallis $p = 0.024$): in AD patients and in MD patients, it was lower compared to "non-neurodegenerative" patients (Mann-Whitney $p = 0.009$ and 0.006, respectively). A summary of imaging-based markers stratified according to etiological subgroups is given in Table 1.

HippForm-FDG was not associated with AD-FDG ($r = 0.107$, $p = 0.322$), but it showed a moderate positive correlation with GM volume of the ipsilateral hippocampal formation ($r = 0.443$, $p < 0.0005$).

3.2. Comparison with cognitively NC subjects

Histograms of HippForm-GM and HippForm-FDG in the sample of cognitively NC subjects compared to the sample of cognitively impaired patients are shown in Fig. 1. HippForm-GM was significantly lower in the cognitively impaired patients compared to the cognitively NCs: 5.38 ± 1.02 mL versus 6.87 ± 0.87 mL ($p < 0.0005$). The difference of the variance (1.02 mL vs. 0.87 mL) did not reach statistical significance (Levene test $p = 0.115$). In contrast, HippForm-FDG was not different between cognitively impaired patients and the cognitively NCs (1.17 ± 0.15 vs. 1.20 ± 0.10, $p = 0.178$). However, the variance was significantly larger in the cognitively impaired patients (0.15 vs. 0.10, $p = 0.001$). The larger variance of HippForm-FDG in the cognitively impaired patients was driven by a rather symmetric broadening of the distribution in both directions (Fig. 1) indicating that there were both cognitively impaired patients with reduced glucose metabolism in the hippocampal formation and cognitively impaired patients with increased glucose metabolism in the hippocampal formation.

3.3. Association between imaging-based markers and cognitive performance in cognitively impaired patients

There was a significant negative correlation between HippForm-FDG and the naming animals z-score ($r = -0.284$, $p = 0.008$) and the S-words z-score ($r = -0.264$, $p = 0.015$) of the CERAD-Plus test battery (Figs. 2 and 3). MRI and PET images of a representative patient are shown in Fig. 4.

Replacing maximum HippForm-FDG of both hemispheres by the mean of both hemispheres resulted in slightly weaker and slightly less significant correlations: the Pearson correlation coefficient between HippForm-FDG and the naming animals z-score changed

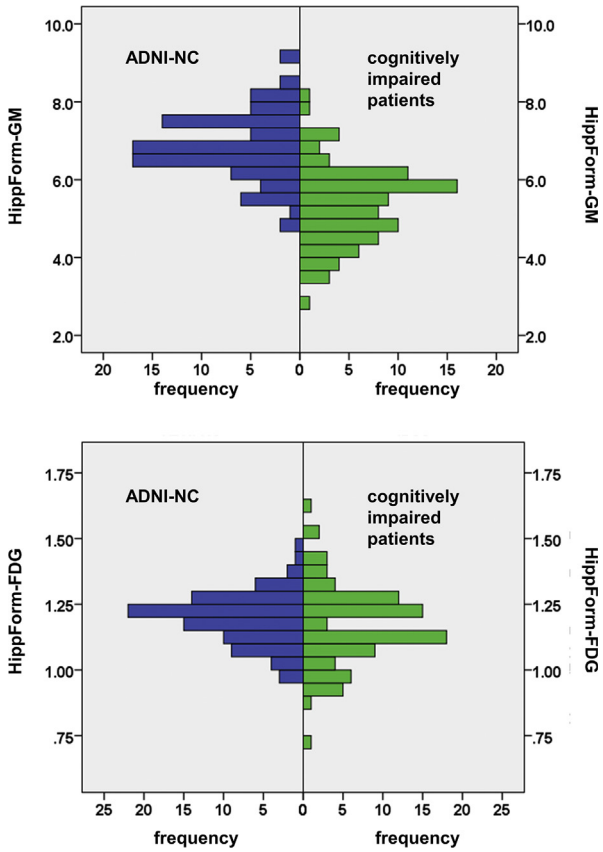

Fig. 1. Histogram of gray matter volume (minimum of both hemispheres, top) and pons-scaled, PVE-corrected FDG uptake (maximum of both hemispheres, bottom) in the hippocampal formation in the cognitively normal controls from the Alzheimer's Disease Neuroimaging initiative (ADNI-NCs, left) compared to the sample of cognitively impaired patients (right). Abbreviations: 18F-FDG, fluorodeoxyglucose; ADNI, Alzheimer's Disease Neuroimaging Initiative; HippForm-FDG, FDG uptake in the hippocampal formation; HippForm-GM, GM volume of the hippocampal formation; PVE, partial volume effect.

from r = −0.284 (p = 0.008) to r = −0.268 (p = 0.013) and the correlation coefficient with the S-words z-score changed from r = −0.264 (p = 0.015) to r = −0.213 (p = 0.052). This suggests that averaging HippForm-FDG over both hemispheres resulted in a small loss of variability of interest.

The negative correlation between HippForm-FDG and the naming animals z-score observed in the whole sample was confirmed in the subsample of patients with AD (either alone or with concomitant CVD, n = 42, r = −0.350, p = 0.025) and in the patients without AD (n = 45, r = −0.328, p = 0.028). Thus, the negative correlation between glucose metabolism in the hippocampal formation and the naming animals z-score was not driven by differences between patients with AD and patients without. This is also evident from the scatter plots in Fig. 3 (top row, left panel): the scatter plot of patients with AD and the scatter plot of patients without AD are fully aligned.

AD-FDG was positively correlated with most of the CERAD-Plus subscores, the correlation was most significant with the MMSE (r = 0.302, p = 0.004, Fig. 2). HippForm-GM was positively correlated with MMSE (r = 0.227, p = 0.034), word list learning (r = 0.272, p = 0.011), word list recall (r = 0.445, p < 0.0005), and figures recall (r = 0.230, p = 0.035).

The positive correlation between AD-FDG and the naming animals z-score observed in the whole sample was not confirmed in the subsample of patients with AD (n = 42, r = 0.065, p = 0.688) nor in the subsample of patients without AD (n = 45, r = 0.151, p = 0.321). Thus, the correlation in the whole sample was mainly driven by differences between patients with and without AD. This is also evident from the scatter plots in Fig. 3 (top row, middle panel): the scatter plot of patients with AD is shifted to bottom left relative to the scatter plot of patients without AD.

The association between HippForm-FDG and the CERAD-Plus animals z-score was confirmed (Table 2) by the partial correlation analyses that corrected for MMSE (partial correlation coefficient between HippForm-FDG and the naming animals z-score r = −0.297, p = 0.006), for AD-FDG (r = −0.334, p = 0.002), or for presence versus absence of clinical AD (r = −0.321, p = 0.003). The negative correlation between HippForm-FDG and the naming animals z-score also remained significant after correction for GM volume of the ipsilateral hippocampal formation (partial correlation coefficient = −0.333, p = 0.002).

Linear regression of the CERAD-Plus animals z-score with HippForm-FDG, AD-FDG, HippForm-GM, and MMSE z-score as explanatory variables included only HippForm-FDG (beta = −0.308, p = 0.003) and the MMSE z-score (beta = 0.382, p < 0.0005) in the final model. AD-FDG (beta = 0.143, p = 0.148) and HippForm-GM (beta = 0.085, p = 0.409) were excluded.

To test for potential impact of the reference region used for scaling of the PET intensity, the correlation analyses were repeated with the cerebellum as PET reference region (instead of the pons). There was a strong correlation between PVE-corrected HippForm-FDG scaled to pons (maximum of both hemispheres) and PVE-corrected HippForm-FDG scaled to cerebellum (maximum of both hemispheres, Pearson correlation coefficient r = 0.862, p < 0.0005). In line with this, the results with the cerebellum as reference region confirmed the results with pons scaling. For example, PVE-corrected HippForm-FDG (maximum of both hemispheres) scaled to the cerebellum also showed a significant negative correlation with the naming animals z-score of the CERAD-Plus test battery (r = −0.299, p = 0.005). This suggests that the negative correlation between glucose metabolism in the hippocampal formation and verbal semantic fluency is not a scaling artifact. Intensity scaling of FDG PET is not required when the absolute local metabolic rate of glucose is determined (in μmol glucose per 100g of tissue per minute). This, however, requires sampling of arterial blood (or arterialized venous blood) starting at the time of FDG administration until the end of the PET scan for computation of the arterial input function for tracer kinetic modeling. Blood sampling during PET had not been performed in the hospitalized geriatric patient sample of this study.

3.4. Association between metabolic activity and connectivity of the hippocampal formation in cognitively impaired patients

Eigenvector centrality of the hippocampal formation (with maximum FDG uptake of left and right hemisphere) was 0.00411 ± 0.00004. It was not correlated with HippForm-FDG (r = −0.087, p = 0.436). HippForm-FDG was also not correlated with functional connectivity of the hippocampal formation (with maximum FDG uptake) with any other AAL-ROI, including the ipsilateral precuneus (r = 0.064, p = 0.569) and the ipsilateral posterior cingulate cortex (r = −0.096, p = 0.393).

Eigenvector centrality of the hippocampal formation (with maximum FDG uptake of left and right hemisphere) was lower in patients with AD (either alone or with concomitant CVD) compared to patients without AD (0.00410 ± 0.00005 vs. 0.00413 ± 0.00003, t test p = 0.011).

4. Discussion

Volume loss of the mesiotemporal lobe is the strongest macrostructural correlate of memory decline in many diseases. In

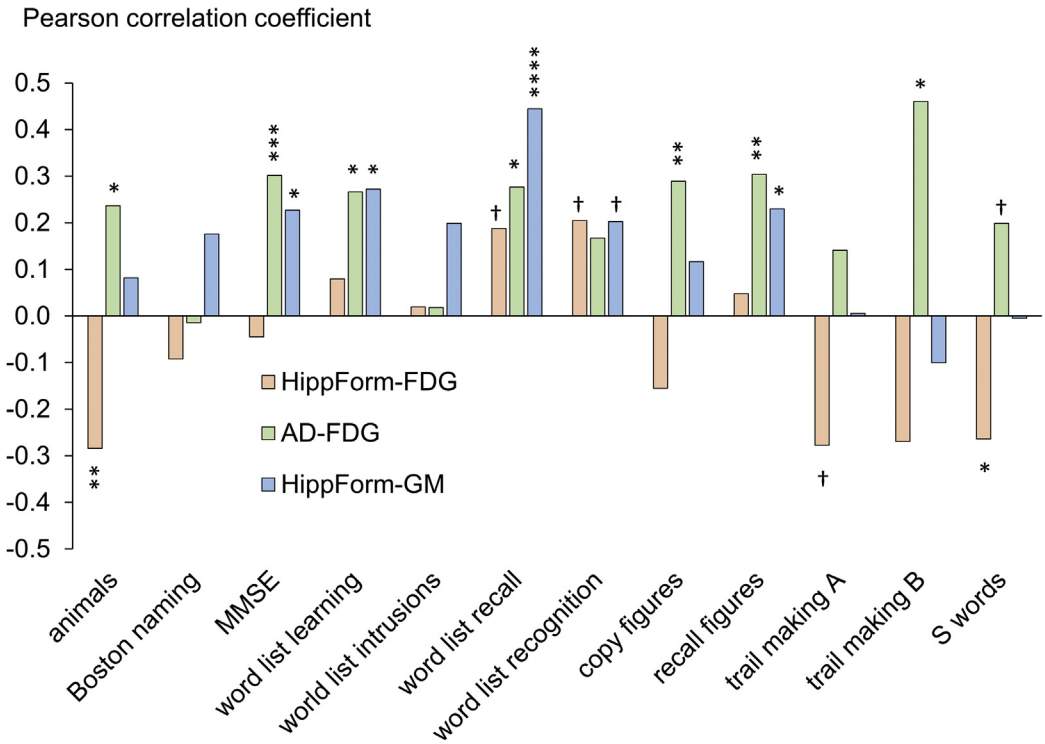

Fig. 2. Pearson coefficient of the correlation between the performance in the different CERAD subdomains (z-scores adjusted for age, gender and education) and pons-scaled, PVE-corrected FDG uptake in the hippocampal formation (HippForm-FDG, maximum of both hemispheres, red), pons-scaled, PVE-corrected FDG uptake in the bilateral AD meta-ROI (AD-FDG, green), and gray matter volume in the hippocampal formation (HippForm-GM, minimum of both hemispheres, blue), * $p < 0.05$, ** $p < 0.01$, *** $p < 0.005$, **** $p < 0.0005$, † $p < 0.10$. Abbreviations: AD, Alzheimer's disease; CERAD, Consortium to Establish a Registry for Alzheimer's Disease; 18F-FDG, fluorodeoxyglucose; PVE, partial volume effect; ROI, region of interest. (For interpretation of the references to color in this figure legend, the reader is referred to the Web version of this article.)

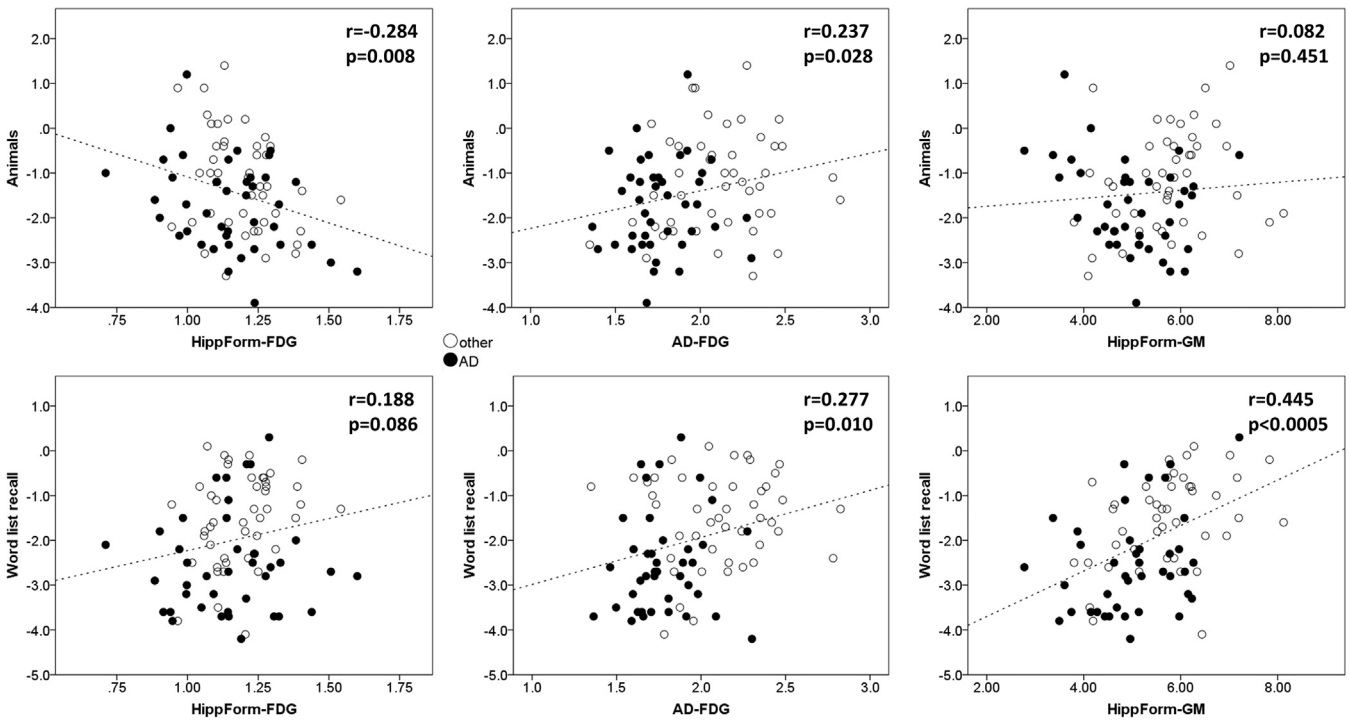

Fig. 3. Scatter plots of the age-, gender-, and education-adjusted z-score of the animals (top) and the word list recall (bottom) subtest of the CERAD test battery versus pons-scaled, PVE-corrected FDG uptake in the hippocampal formation (HippForm-FDG, maximum of both hemispheres, left column), pons-scaled, PVE-corrected FDG uptake in the bilateral AD meta-ROI (AD-FDG, middle column), and gray matter volume in the hippocampal formation (HippForm-GM, minimum of both hemispheres, right column). Filled symbol: patients with clinical AD, either alone or with concomitant cerebrovascular disease; Open symbol: cases without clinical AD; and Dashed line: linear regression. Abbreviations: AD, Alzheimer's disease; CERAD, Consortium to Establish a Registry for Alzheimer's Disease; 18F-FDG, fluorodeoxyglucose; PVE, partial volume effect; ROI, region of interest.

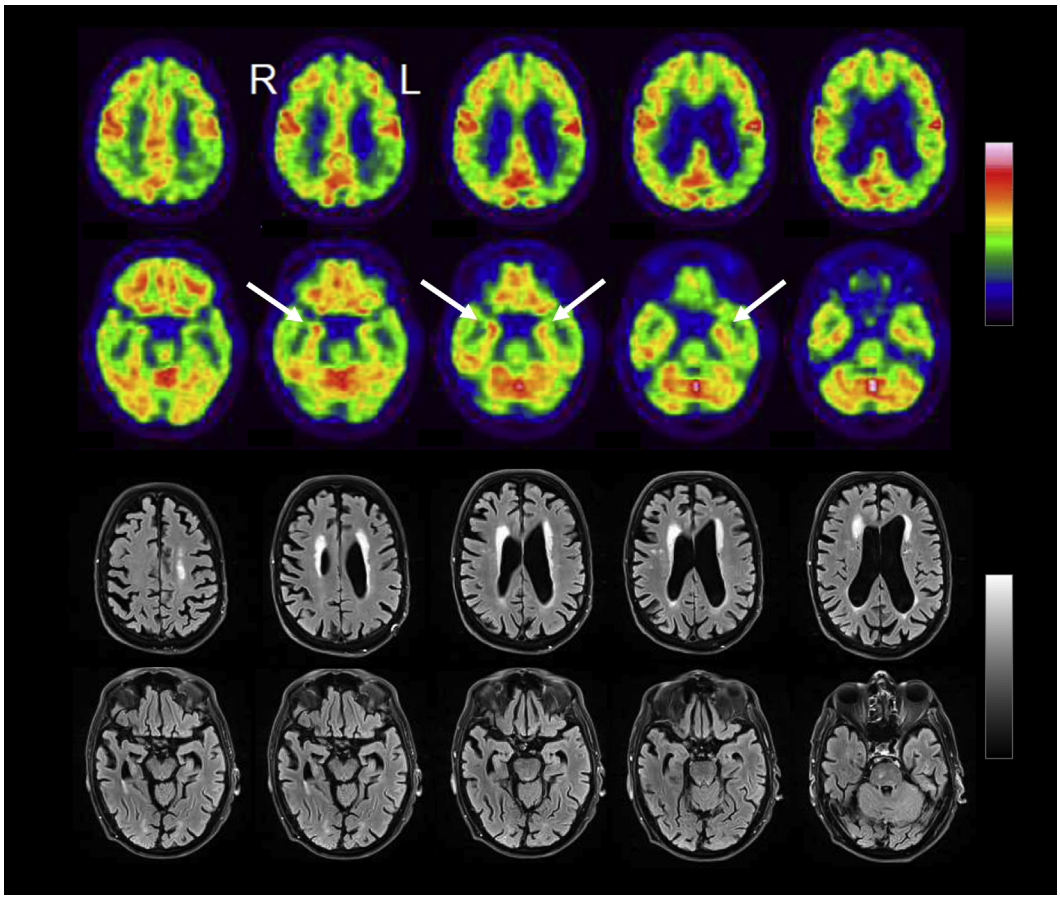

Fig. 4. A 77-year-old male patient with first diagnosis of mild dementia probably due to MD: CDR = 1, MMSE = 19 (z = −5.2), and CERAD-Plus animals z = −3.2. Reduced FDG uptake in Alzheimer's disease characteristic brain regions (posterior cingulate and parietotemporal association cortex) and relatively high FDG uptake in mesiotemporal lobe including the hippocampal formation (arrows). MRI shows considerable white matter hyperintensities and mesiotemporal atrophy. Abbreviations: CDR, Clinical Dementia Rating; CERAD, Consortium to Establish a Registry for Alzheimer's Disease; MMSE, Mini–Mental State Examination.

contrast, glucose metabolism in the mesiotemporal lobe can be relatively preserved or even increased also at advanced disease stages (Chetelat et al., 2008; Ishii et al., 1998; Tahmasian et al., 2015). Possible explanations include compensatory (beneficial) recruitment of additional neuronal resources (Chetelat et al., 2008) and maladaptive overactivity ("running hot") of internal hippocampal circuitry (Bakker et al., 2012; Das et al., 2013; Salami et al., 2014; Tahmasian et al., 2015). In the first case (beneficial compensation), hippocampal glucose metabolism is expected to be positively correlated with cognitive performance. In the latter case (maladaptive overactivity) the correlation is expected to be negative.

The main finding of the present study is the *negative* correlation between glucose metabolism in the hippocampal formation and cognitive performance in several domains in cognitively impaired patients, that is, higher glucose metabolism in the hippocampal formation was associated with poorer cognitive performance. This suggests that increased glucose metabolism in the hippocampal formation of cognitively impaired patients is a consequence of detrimental adaption rather than a beneficial compensatory reaction. The association between higher glucose metabolism in the hippocampal formation and lower CERAD-Plus scores was most significant statistically for the naming animals subscore. In the naming animals test, subjects are asked to name as many animals as possible in 60 seconds. The performance in this test depends on language, verbal productivity, semantic memory, and cognitive flexibility. The association between higher glucose metabolism in the hippocampal formation and lower verbal semantic fluency was independent of the magnitude of overall neuronal dysfunction/degeneration as measured by hypometabolism in AD characteristic brain regions (Table 2). It was also independent of the presence (vs. absence) of clinical Alzheimer's disease (Table 2, Fig. 3). This suggests that the association between higher glucose metabolism in the hippocampal formation and lower verbal semantic fluency is not specific for AD (similar to the association between mesiotemporal atrophy and memory performance i.e., also not specific for AD). In line with this, glucose metabolism in the hippocampal formation did not differ between the different etiological subgroups of cognitively impaired patients. Finally, the association was also independent of overall cognitive performance (MMSE), indicating that it is specific for verbal semantic fluency to some extent. This is in line with the well-documented role of hippocampal integrity for verbal semantic fluency (Baldo et al., 2006; Gleissner and Elger, 2001; Glikmann-Johnston et al., 2015).

PVE-corrected HippForm-FDG was significantly correlated with its GM volume ($r = 0.443$, $p < 0.005$). Thus, it might not be excluded a priori that the observed negative correlation between PVE-corrected HippForm-FDG and the CERAD-Plus animals z-score was driven by GM volume, for example, due to incomplete correction or overcorrection of PVEs by the used Müller-Gärtner method. However, the negative correlation remained significant also after correction for GM volume of the ipsilateral hippocampal formation, suggesting that it is independent of GM volume. This was further supported by linear regression of the naming animals

Table 2
Partial correlation between pons-scaled, PVE-corrected HippForm-FDG (maximum over both hemispheres) and the different CERAD-Plus subdomains (z-scores adjusted for age, gender, and education) corrected for overall cognitive performance (MMSE z-score), for pons-scaled, PVE-corrected FDG uptake in the AD meta-ROI, or for presence versus absence of clinical Alzheimer's disease

CERAD-Plus (z-score)	HippForm-FDG corrected for MMSE	HippForm-FDG corrected for AD-FDG	HippForm-FDG corrected for Alzheimer's disease
Animals	−0.297	−0.334	−0.321
p	0.006	0.002	0.003
Boston Naming Test	−0.084	−0.102	−0.091
p	0.451	0.359	0.413
MMSE	–	−0.089	−0.082
p		0.417	0.455
Learning word list	0.132	0.045	0.054
p	0.230	0.682	0.626
Word list intrusions	0.024	0.004	0.018
p	0.828	0.969	0.872
Recall word list	0.270	0.143	0.165
p	0.013	0.194	0.133
Word list recognition	0.232	0.184	0.191
p	0.033	0.095	0.082
Copy figures	−0.149	−0.168	−0.196
p	0.180	0.129	0.076
Recall figures	0.079	0.017	0.016
p	0.476	0.879	0.885
Trail Making Test A	−0.224	−0.264	−0.246
p	0.066	0.029	0.043
Trail Making Test B	−0.268	−0.314	−0.360
p	0.186	0.118	0.071
S-words	−0.266	−0.290	−0.293
p	0.015	0.008	0.007

Given are the partial correlation coefficients together with their *p*-value.
Key: AD, Alzheimer's disease; CERAD, Consortium to Establish a Registry for Alzheimer's Disease; FDG, 18F-fluorodeoxyglucose; HippForm-FDG, FDG uptake in the hippocampal formation; MMSE, Mini–Mental State Examination; ROI, region of interest.

z-score with PVE-corrected HippForm-FDG, PVE-corrected FDG uptake in the AD signature-ROI, HippForm-GM, and MMSE z-score as explanatory variables. The final model included PVE-corrected HippForm-FDG and the MMSE z-score, but neither PVE-corrected FDG uptake in the AD signature-ROI nor HippForm-GM.

Integrity of the hippocampal formation is most consistently associated with short-term episodic memory. In line with this, HippForm-GM was positively correlated with recall measures of the CERAD-Plus test battery, most pronounced with word list recall (Figs. 2 and 3). That is, atrophy of the hippocampal formation was associated with impaired word list recall. Concerning the association of PVE-corrected FDG uptake in AD-typical brain regions with cognitive performance, the most significant effect was a positive correlation with overall cognitive performance as measured by the MMSE z-score. PVE-corrected FDG uptake in AD-typical brain regions was positively correlated also with the naming animals z-score, in clear contrast to the negative correlation of PVE-corrected HippForm-FDG with the naming animals z-score. Furthermore, when the correlation between PVE-corrected HippForm-FDG and the naming animals z-score was corrected for PVE-corrected FDG uptake in AD-typical brain regions, the correlation became slightly stronger and slightly more significant (partial correlation coefficient = −0.334, $p = 0.002$, vs. Pearson correlation coefficient r = −0.284, $p = 0.008$ without correction). Taken together, these findings suggest that the observed negative correlation between glucose metabolism in the hippocampal formation and verbal semantic fluency is caused by a mechanism that is independent of hippocampal atrophy and AD-typical cortical hypometabolism.

The present study extends previous findings of Pasquini et al. who reported increased intrinsic functional connectivity of the hippocampus in patients with AD to be associated with more strongly impaired delayed recall (Pasquini et al., 2015). Therapeutic potential was demonstrated by Bakker et al. who used low-dose levetiracetam, an antiepileptic drug, to target excess hippocampal activity in patients with amnestic MCI (Bakker et al., 2012). Two weeks of treatment reduced hippocampal activity toward normal values and significantly improved memory function in a three-choice memory task (Bakker et al., 2012). It is important to mention that Bakker et al. characterized hippocampal activity by fMRI measurement of the blood oxygenation level dependent response during a cognitive task designed to assess memory errors (Bakker et al., 2012). The results need not necessarily apply to mesiotemporal hyperactivity in resting state as characterized by glucose metabolism in FDG PET. Considering the risk of unwanted side effects, the therapeutic potential of low-dose levetiracetam in patients with cognitive impairment and increased glucose metabolism in the hippocampal formation should be tested in a prospective study before it might be recommended for clinical use.

There is evidence from preclinical studies that tau pathology interferes with the regulation of excitability and synchronization of neuronal networks. Genetic removal of tau decreases hyperexcitability in animal models of epilepsy resulting in reduced interictal spiking and spontaneous seizures (Holth et al., 2013; Roberson et al., 2007), it normalizes inhibitory/excitatory imbalance (Roberson et al., 2007, 2011), and it rescues long-term potentiation alterations in AD mouse models (Shipton et al., 2011). Disruption of GABAergic neuronal networks is one possible mechanism of tau-associated disturbance of excitability of hippocampal neurons (Levenga et al., 2013; Loreth et al., 2012), as the alterations can be reversed by GABA-A receptor agonists (Levenga et al., 2013). Thus, tau-related disruption of GABAergic neuronal networks is a potential mechanism of hippocampal hyperactivity as measured by FDG PET in cognitive impaired elderly.

The present study did not find increased hippocampal glucose metabolism to be associated with decreased connectivity of the hippocampus to other brain regions. Tahmasian et al., using very similar methods for data analysis of both FDG PET and rs-fMRI, found a negative correlation between hippocampal glucose metabolism and functional connectivity of the hippocampus and precuneus in 40 patients with AD dementia (mean MMSE = 22; partial correlation coefficient corrected for age, sex, GM volume in the hippocampus, and GM volume in the precuneus = −0.275, $p = 0.050$; Tahmasian et al., 2015). However, there was no correlation in the 21 MCI patients included in that study (mean MMSE = 27, partial correlation coefficient = −0.036, $p = 0.44$; Tahmasian et al., 2015). Thus, the lack of significant correlation between glucose metabolism of the hippocampal formation and its functional connectivity to other brain regions in the present study might be explained by the more heterogeneous patient sample, both with respect to the severity of cognitive impairment (ranging from MCI to moderate dementia) and with respect to its etiology: non-neurodegenerative etiology (e.g., reduced general health, depression, and prolonged effect of delirium), AD, CVD, MD, and neurodegenerative etiology other than AD (e.g., Lewy body disease and frontotemporal lobar degeneration). In addition, the patient sample of the present study included a rather large fraction of patients with considerable WM disease that might affect functional connectivity. Scoring of the severity of WM hyperintensity burden by an experienced neuroradiologist had resulted in "mild, normal for age" in 37 patients (42.5%), "moderate, more than expected for age" in 34 patients (39.1%), and "extensive" in 16 patients (18.4%). Furthermore, Tahmasian et al. used an integrated PET/MRI system for simultaneous acquisition of FDG PET and rs-fMRI (Tahmasian et al., 2015). In the present study, PET and rs-fMRI had been performed with 2 different scanners on 2 different days. Although the delay

between PET and fMRI was rather small (no more than 1 week in 82 of the 87 patients and no more than 1 month in the remaining 5 patients), it might have caused additional variability that reduced the power to detect associations between cerebral glucose metabolism and functional connectivity. Given that spatial overlap and quantitative correlation of FDG uptake and functional connectivity is surprisingly low in many studies (Adriaanse et al., 2016; despite the expected causal relationship between synaptic failure and impaired functional connectivity), this additional variability might have obscured potential associations in the present study. Finally, it is important to mention that acute phase autoimmune encephalitis that can be associated with mesiotemporal hypermetabolism (limbic encephalitis), particularly in patients with autoantibodies against intracellular antigens (Baumgartner et al., 2013), was very unlikely in the patients of the present study, although chronic phase autoimmune encephalitis is increasingly recognized as possible explanation of clinically uncertain cognitive decline in the elderly (Doss et al., 2014).

In conclusion, the findings of the present study provide evidence that increased glucose metabolism in the hippocampal formation of cognitively impaired patients is a consequence of detrimental adaption rather than a beneficial compensatory reaction. Thus, excess glucose metabolism of the hippocampal formation might be a useful therapeutic target in these patients.

Disclosure statement

The authors have no actual or potential conflicts of interest.

Acknowledgements

Data collection and sharing for this project was funded by the Alzheimer's Disease Neuroimaging Initiative (ADNI; National Institutes of Health Grant U01 AG024904) and DOD ADNI (Department of Defense award number W81XWH-12-2-0012). ADNI is funded by the National Institute on Aging, the National Institute of Biomedical Imaging and Bioengineering, and through generous contributions from the following: AbbVie; Alzheimer's Association; Alzheimer's Drug Discovery Foundation; Araclon Biotech; BioClinica, Inc; Biogen; Bristol-Myers Squibb Company; CereSpir, Inc; Cogstate; Eisai Inc; Elan Pharmaceuticals, Inc; Eli Lilly and Company; EuroImmun; F. Hoffmann-La Roche Ltd and its affiliated company Genentech, Inc; Fujirebio; GE Healthcare; IXICO Ltd.; Janssen Alzheimer Immunotherapy Research & Development, LLC.; Johnson & Johnson Pharmaceutical Research & Development LLC.; Lumosity; Lundbeck; Merck & Co, Inc; Meso Scale Diagnostics, LLC.; NeuroRx Research; Neurotrack Technologies; Novartis Pharmaceuticals Corporation; Pfizer Inc; Piramal Imaging; Servier; Takeda Pharmaceutical Company; and Transition Therapeutics. The Canadian Institutes of Health Research is providing funds to support ADNI clinical sites in Canada. Private sector contributions are facilitated by the Foundation for the National Institutes of Health (www.fnih.org). The grantee organization is the Northern California Institute for Research and Education, and the study is coordinated by the Alzheimer's Therapeutic Research Institute at the University of Southern California. ADNI data are disseminated by the Laboratory for Neuro Imaging at the University of Southern California.

This work was supported by the Regional Development Fund of the European Union (reference numbers 10153407, 10153971, 10153458, 10153460, 10153461, 10153462, and 10153463).

References

Adriaanse, S.M., Wink, A.M., Tijms, B.M., Ossenkoppele, R., Verfaillie, S.C., Lammertsma, A.A., Boellaard, R., Scheltens, P., van Berckel, B.N., Barkhof, F., 2016. The association of glucose metabolism and eigenvector centrality in Alzheimer's disease. Brain Connect. 6, 1–8.

Apostolova, I., Lange, C., Roberts, A., Igel, H.J., Maurer, A., Liese, S., Estrella, M., Prasad, V., Stechl, E., Lammler, G., Steinhagen-Thiessen, E., Buchert, R., 2017. Challenges in screening and recruitment for a neuroimaging study in cognitively impaired geriatric inpatients. J. Alzheimers Dis. 56, 197–204.

Bakker, A., Krauss, G.L., Albert, M.S., Speck, C.L., Jones, L.R., Stark, C.E., Yassa, M.A., Bassett, S.S., Shelton, A.L., Gallagher, M., 2012. Reduction of hippocampal hyperactivity improves cognition in amnestic mild cognitive impairment. Neuron 74, 467–474.

Baldo, J.V., Schwartz, S., Wilkins, D., Dronkers, N.F., 2006. Role of frontal versus temporal cortex in verbal fluency as revealed by voxel-based lesion symptom mapping. J. Int. Neuropsychol. Soc. 12, 896–900.

Baumgartner, A., Rauer, S., Mader, I., Meyer, P.T., 2013. Cerebral FDG-PET and MRI findings in autoimmune limbic encephalitis: correlation with autoantibody types. J. Neurol. 260, 2744–2753.

Behzadi, Y., Restom, K., Liau, J., Liu, T.T., 2007. A component based noise correction method (CompCor) for BOLD and perfusion based fMRI. Neuroimage 37, 90–101.

Braak, H., Braak, E., 1991. Neuropathological stageing of Alzheimer-related changes. Acta Neuropathologica 82, 239–259.

Brier, M.R., Thomas, J.B., Snyder, A.Z., Benzinger, T.L., Zhang, D., Raichle, M.E., Holtzman, D.M., Morris, J.C., Ances, B.M., 2012. Loss of intranetwork and internetwork resting state functional connections with Alzheimer's disease progression. J. Soc. Neurosci. 32, 8890–8899.

Chapleau, M., Aldebert, J., Montembeault, M., Brambati, S.M., 2016. Atrophy in Alzheimer's disease and semantic dementia: an ALE meta-analysis of voxel-based morphometry studies. J. Alzheimers Dis. 54, 941–955.

Chetelat, G., Desgranges, B., Landeau, B., Mezenge, F., Poline, J.B., de la Sayette, V., Viader, F., Eustache, F., Baron, J.C., 2008. Direct voxel-based comparison between grey matter hypometabolism and atrophy in Alzheimer's disease. Brain 131 (Pt 1), 60–71.

Das, S.R., Pluta, J., Mancuso, L., Kliot, D., Orozco, S., Dickerson, B.C., Yushkevich, P.A., Wolk, D.A., 2013. Increased functional connectivity within medial temporal lobe in mild cognitive impairment. Hippocampus 23, 1–6.

De Santi, S., de Leon, M.J., Rusinek, H., Convit, A., Tarshish, C.Y., Roche, A., Tsui, W.H., Kandil, E., Boppana, M., Daisley, K., Wang, G.J., Schlyer, D., Fowler, J., 2001. Hippocampal formation glucose metabolism and volume losses in MCI and AD. Neurobiol. Aging 22, 529–539.

den Heijer, T., Tiemeier, H., Luijendijk, H.J., van der Lijn, F., Koudstaal, P.J., Hofman, A., Breteler, M.M., 2011. A study of the bidirectional association between hippocampal volume on magnetic resonance imaging and depression in the elderly. Biol. Psychiatry 70, 191–197.

Dermody, N., Hornberger, M., Piguet, O., Hodges, J.R., Irish, M., 2016. Prospective memory impairments in Alzheimer's disease and behavioral variant frontotemporal dementia: clinical and neural correlates. J. Alzheimers Dis. 50, 425–441.

Desgranges, B., Baron, J.C., de la Sayette, V., Petit-Taboue, M.C., Benali, K., Landeau, B., Lechevalier, B., Eustache, F., 1998. The neural substrates of memory systems impairment in Alzheimer's disease. A PET study of resting brain glucose utilization. Brain 121 (Pt 4), 611–631.

DiFeo, G., Shors, T.J., 2017. Mental and physical skill training increases neurogenesis via cell survival in the adolescent hippocampus. Brain Res. 1654 (Pt B), 95–101.

Doss, S., Wandinger, K.P., Hyman, B.T., Panzer, J.A., Synofzik, M., Dickerson, B., Mollenhauer, B., Scherzer, C.R., Ivinson, A.J., Finke, C., Schols, L., Muller Vom Hagen, J., Trenkwalder, C., Jahn, H., Holtje, M., Biswal, B.B., Harms, L., Ruprecht, K., Buchert, R., Hoglinger, G.U., Oertel, W.H., Unger, M.M., Kortvelyessy, P., Bittner, D., Priller, J., Spruth, E.J., Paul, F., Meisel, A., Lynch, D.R., Dirnagl, U., Endres, M., Teegen, B., Probst, C., Komorowski, L., Stocker, W., Dalmau, J., Pruss, H., 2014. High prevalence of NMDA receptor IgA/IgM antibodies in different dementia types. Ann. Clin. Transl. Neurol. 1, 822–832.

Duzel, E., van Praag, H., Sendtner, M., 2016. Can physical exercise in old age improve memory and hippocampal function? Brain 139 (Pt 3), 662–673.

Ehrensperger, M.M., Berres, M., Taylor, K.I., Monsch, A.U., 2010. Early detection of Alzheimer's disease with a total score of the German CERAD. J. Int. Neuropsychol. Soc. 16, 910–920.

Gee, M., Dukart, J., Draganski, B., Wayne Martin, W.R., Emery, D., Camicioli, R., 2017. Regional volumetric change in Parkinson's disease with cognitive decline. J. Neurol. Sci. 373, 88–94.

Gleissner, U., Elger, C.E., 2001. The hippocampal contribution to verbal fluency in patients with temporal lobe epilepsy. Cortex 37, 55–63.

Glikmann-Johnston, Y., Oren, N., Hendler, T., Shapira-Lichter, I., 2015. Distinct functional connectivity of the hippocampus during semantic and phonemic fluency. Neuropsychologia 69, 39–49.

Gonzalez-Escamilla, G., Lange, C., Teipel, S., Buchert, R., Grothe, M.J. Alzheimer's Disease Neuroimaging, I., 2017. PETPVE12: an SPM toolbox for Partial Volume Effects correction in brain PET - Application to amyloid imaging with AV45-PET. Neuroimage 147, 669–677.

Herholz, K., Salmon, E., Perani, D., Baron, J.C., Holthoff, V., Frolich, L., Schonknecht, P., Ito, K., Mielke, R., Kalbe, E., Zundorf, G., Delbeuck, X., Pelati, O., Anchisi, D., Fazio, F., Kerrouche, N., Desgranges, B., Eustache, F., Beuthien-Baumann, B., Menzel, C., Schroder, J., Kato, T., Arahata, Y., Henze, M., Heiss, W.D., 2002. Discrimination between Alzheimer dementia and controls by automated analysis of multicenter FDG PET. Neuroimage 17, 302–316.

Holth, J.K., Bomben, V.C., Reed, J.G., Inoue, T., Younkin, L., Younkin, S.G., Pautler, R.G., Botas, J., Noebels, J.L., 2013. Tau loss attenuates neuronal network hyperexcitability in mouse and Drosophila genetic models of epilepsy. J. Soc. Neurosci. 33, 1651–1659.

Ibanez, V., Pietrini, P., Alexander, G.E., Furey, M.L., Teichberg, D., Rajapakse, J.C., Rapoport, S.I., Schapiro, M.B., Horwitz, B., 1998. Regional glucose metabolic abnormalities are not the result of atrophy in Alzheimer's disease. Neurology 50, 1585–1593.

Ishii, K., Kitagaki, H., Kono, M., Mori, E., 1996. Decreased medial temporal oxygen metabolism in Alzheimer's disease shown by PET. J. Nucl. Med. 37, 1159–1165.

Ishii, K., Sasaki, M., Yamaji, S., Sakamoto, S., Kitagaki, H., Mori, E., 1998. Relatively preserved hippocampal glucose metabolism in mild Alzheimer's disease. Dement. Geriatr. Cogn. Disord. 9, 317–322.

Jack Jr., C.R., Petersen, R.C., Xu, Y.C., O'Brien, P.C., Smith, G.E., Ivnik, R.J., Boeve, B.F., Waring, S.C., Tangalos, E.G., Kokmen, E., 1999. Prediction of AD with MRI-based hippocampal volume in mild cognitive impairment. Neurology 52, 1397–1403.

Jagust, W.J., Bandy, D., Chen, K., Foster, N.L., Landau, S.M., Mathis, C.A., Price, J.C., Reiman, E.M., Skovronsky, D., Koeppe, R.A. Alzheimer's Disease Neuroimaging, I., 2010. The Alzheimer's Disease Neuroimaging Initiative positron emission tomography core. Alzheimer's Dement. 6, 221–229.

Joshi, A., Koeppe, R.A., Fessler, J.A., 2009. Reducing between scanner differences in multi-center PET studies. Neuroimage 46, 154–159.

Lange, C., Suppa, P., Frings, L., Brenner, W., Spies, L., Buchert, R., 2016. Optimization of statistical single subject analysis of brain FDG PET for the prognosis of mild cognitive impairment-to-Alzheimer's disease conversion. J. Alzheimers Dis. 49, 945–959.

Levenga, J., Krishnamurthy, P., Rajamohamedsait, H., Wong, H., Franke, T.F., Cain, P., Sigurdsson, E.M., Hoeffer, C.A., 2013. Tau pathology induces loss of GABAergic interneurons leading to altered synaptic plasticity and behavioral impairments. Acta Neuropathol. Commun. 1, 34.

Lohmann, G., Margulies, D.S., Horstmann, A., Pleger, B., Lepsien, J., Goldhahn, D., Schloegl, H., Stumvoll, M., Villringer, A., Turner, R., 2010. Eigenvector centrality mapping for analyzing connectivity patterns in fMRI data of the human brain. PLoS One 5, e10232.

Loreth, D., Ozmen, L., Revel, F.G., Knoflach, F., Wetzel, P., Frotscher, M., Metzger, F., Kretz, O., 2012. Selective degeneration of septal and hippocampal GABAergic neurons in a mouse model of amyloidosis and tauopathy. Neurobiol. Dis. 47, 1–12.

Maldjian, J.A., Laurienti, P.J., Kraft, R.A., Burdette, J.H., 2003. An automated method for neuroanatomic and cytoarchitectonic atlas-based interrogation of fMRI data sets. Neuroimage 19, 1233–1239.

Minoshima, S., Frey, K.A., Foster, N.L., Kuhl, D.E., 1995. Preserved pontine glucose metabolism in Alzheimer disease: a reference region for functional brain image (PET) analysis. J. Comput. Assist. Tomogr. 19, 541–547.

Minoshima, S., Giordani, B., Berent, S., Frey, K.A., Foster, N.L., Kuhl, D.E., 1997. Metabolic reduction in the posterior cingulate cortex in very early Alzheimer's disease. Ann. Neurol. 42, 85–94.

Monsch, A.U., Kressig, R.W., 2010. Specific care program for the older adults: memory clinics. Eur. Geriatr. Med. 1, 128–131.

Morris, J.C., Mohs, R.C., Rogers, H., Fillenbaum, G., Heyman, A., 1988. Consortium to establish a registry for Alzheimer's disease (CERAD) clinical and neuropsychological assessment of Alzheimer's disease. Psychopharmacol. Bull 24, 641–652.

Mosconi, L., Sorbi, S., de Leon, M.J., Li, Y., Nacmias, B., Myoung, P.S., Tsui, W., Ginestroni, A., Bessi, V., Fayyazz, M., Caffarra, P., Pupi, A., 2006. Hypometabolism exceeds atrophy in presymptomatic early-onset familial Alzheimer's disease. J. Nucl. Med. 47, 1778–1786.

Mosconi, L., Tsui, W.H., De Santi, S., Li, J., Rusinek, H., Convit, A., Li, Y., Boppana, M., de Leon, M.J., 2005. Reduced hippocampal metabolism in MCI and AD: automated FDG-PET image analysis. Neurology 64, 1860–1867.

Muller-Gartner, H.W., Links, J.M., Prince, J.L., Bryan, R.N., McVeigh, E., Leal, J.P., Davatzikos, C., Frost, J.J., 1992. Measurement of radiotracer concentration in brain gray matter using positron emission tomography: MRI-based correction for partial volume effects. J. Cereb. Blood Flow Metab. 12, 571–583.

Nestor, P.J., Fryer, T.D., Smielewski, P., Hodges, J.R., 2003. Limbic hypometabolism in Alzheimer's disease and mild cognitive impairment. Ann. Neurol. 54, 343–351.

Pasquini, L., Scherr, M., Tahmasian, M., Meng, C., Myers, N.E., Ortner, M., Muhlau, M., Kurz, A., Forstl, H., Zimmer, C., Grimmer, T., Wohlschlager, A.M., Riedl, V., Sorg, C., 2015. Link between hippocampus' raised local and eased global intrinsic connectivity in AD. J. Alzheimer's Dement. 11, 475–484.

Petrella, J.R., Sheldon, F.C., Prince, S.E., Calhoun, V.D., Doraiswamy, P.M., 2011. Default mode network connectivity in stable vs progressive mild cognitive impairment. Neurology 76, 511–517.

Pievani, M., Filippini, N., van den Heuvel, M.P., Cappa, S.F., Frisoni, G.B., 2014. Brain connectivity in neurodegenerative diseases–from phenotype to proteinopathy. Nature reviews. Neurology 10, 620–633.

Ritter, K., Lange, C., Weygandt, M., Maurer, A., Roberts, A., Estrella, M., Suppa, P., Spies, L., Prasad, V., Steffen, I., Apostolova, I., Bittner, D., Govercin, M., Brenner, W., Mende, C., Peters, O., Seybold, J., Fiebach, J.B., Steinhagen-Thiessen, E., Hampel, H., Haynes, J.D., Buchert, R., 2016. Combination of structural MRI and FDG-PET of the brain improves diagnostic accuracy in newly manifested cognitive impairment in geriatric inpatients. J. Alzheimers Dis. 54, 1319–1331.

Roberson, E.D., Halabisky, B., Yoo, J.W., Yao, J., Chin, J., Yan, F., Wu, T., Hamto, P., Devidze, N., Yu, G.Q., Palop, J.J., Noebels, J.L., Mucke, L., 2011. Amyloid-beta/Fyn-induced synaptic, network, and cognitive impairments depend on tau levels in multiple mouse models of Alzheimer's disease. J. Neurosci. 31, 700–711.

Roberson, E.D., Scearce-Levie, K., Palop, J.J., Yan, F., Cheng, I.H., Wu, T., Gerstein, H., Yu, G.Q., Mucke, L., 2007. Reducing endogenous tau ameliorates amyloid beta-induced deficits in an Alzheimer's disease mouse model. Science 316, 750–754.

Salami, A., Pudas, S., Nyberg, L., 2014. Elevated hippocampal resting-state connectivity underlies deficient neurocognitive function in aging. Proc. Natl. Acad. Sci. U. S. A. 111, 17654–17659.

Schmidt-Kastner, R., Freund, T.F., 1991. Selective vulnerability of the hippocampus in brain ischemia. Neuroscience 40, 599–636.

Schroder, J., Pantel, J., 2016. Neuroimaging of hippocampal atrophy in early recognition of Alzheimer's disease–a critical appraisal after two decades of research. Psychiatry Res. 247, 71–78.

Shipton, O.A., Leitz, J.R., Dworzak, J., Acton, C.E., Tunbridge, E.M., Denk, F., Dawson, H.N., Vitek, M.P., Wade-Martins, R., Paulsen, O., Vargas-Caballero, M., 2011. Tau protein is required for amyloid {beta}-induced impairment of hippocampal long-term potentiation. J. Soc. Neurosci. 31, 1688–1692.

Sokoloff, L., 1999. Energetics of functional activation in neural tissues. Neurochem. Res. 24, 321–329.

Suppa, P., Anker, U., Spies, L., Bopp, I., Ruegger-Frey, B., Klaghofer, R., Gocke, C., Hampel, H., Beck, S., Buchert, R., 2015a. Fully automated atlas-based hippocampal volumetry for detection of Alzheimer's disease in a memory clinic setting. J. Alzheimers Dis. 44, 183–193.

Suppa, P., Hampel, H., Spies, L., Fiebach, J.B., Dubois, B., Buchert, R. Alzheimer's Disease Neuroimaging, I., 2015b. Fully automated atlas-based Hippocampus volumetry for clinical routine: validation in subjects with mild cognitive impairment from the ADNI cohort. J. Alzheimers Dis. 46, 199–209.

Tahmasian, M., Pasquini, L., Scherr, M., Meng, C., Forster, S., Mulej Bratec, S., Shi, K., Yakushev, I., Schwaiger, M., Grimmer, T., Diehl-Schmid, J., Riedl, V., Sorg, C., Drzezga, A., 2015. The lower hippocampus global connectivity, the higher its local metabolism in Alzheimer disease. Neurology 84, 1956–1963.

Ten Kate, M., Barkhof, F., Boccardi, M., Visser, P.J., Jack Jr., C.R., Lovblad, K.O., Frisoni, G.B., Scheltens, P. Geneva Task Force for the Roadmap of Alzheimer's, B., 2017. Clinical validity of medial temporal atrophy as a biomarker for Alzheimer's disease in the context of a structured 5-phase development framework. Neurobiol. Aging 52, 167–182.e161.

Terry, R.D., Masliah, E., Salmon, D.P., Butters, N., DeTeresa, R., Hill, R., Hansen, L.A., Katzman, R., 1991. Physical basis of cognitive alterations in Alzheimer's disease: synapse loss is the major correlate of cognitive impairment. Ann. Neurol. 30, 572–580.

Tzourio-Mazoyer, N., Landeau, B., Papathanassiou, D., Crivello, F., Etard, O., Delcroix, N., Mazoyer, B., Joliot, M., 2002. Automated anatomical labeling of activations in SPM using a macroscopic anatomical parcellation of the MNI MRI single-subject brain. Neuroimage 15, 273–289.

Varrone, A., Asenbaum, S., Vander Borght, T., Booij, J., Nobili, F., Nagren, K., Darcourt, J., Kapucu, O.L., Tatsch, K., Bartenstein, P., Van Laere, K., 2009. EANM procedure guidelines for PET brain imaging using [F-18]FDG, version 2. Eur. J. Nucl. Med. Mol. 36, 2103–2110.

Wink, A.M., de Munck, J.C., van der Werf, Y.D., van den Heuvel, O.A., Barkhof, F., 2012. Fast eigenvector centrality mapping of voxel-wise connectivity in functional magnetic resonance imaging: implementation, validation, and interpretation. Brain Connect. 2, 265–274.

Wolf, D., Bocchetta, M., Preboske, G.M., Boccardi, M., Grothe, M.J. Alzheimer's Disease Neuroimaging, I., 2017. Reference standard space hippocampus labels according to the European Alzheimer's Disease Consortium-Alzheimer's Disease Neuroimaging Initiative harmonized protocol: Utility in automated volumetry. Alzheimer's Demen. 13, 893–902.

Zhang, H.Y., Wang, S.J., Liu, B., Ma, Z.L., Yang, M., Zhang, Z.J., Teng, G.J., 2010. Resting brain connectivity: changes during the progress of Alzheimer disease. Radiology 256, 598–606.